Contribution from the Department of Chemistry,
University of Houston, Houston, Texas 77004

Electrochemistry of (TMP)FeOH and (TMP)$FeOCH_3$ in Dichloromethane. Electrogeneration of Iron(IV) and Iron(II) Porphyrins

C. Swistak, X. H. Mu, and K. M. Kadish*

Received June 26, 1987

The electrochemistry of (TMP)FeOH, (TMP)$FeOCH_3$, and (TMP)FeOR where TMP is the dianion of tetrakis(2,4,6-trimethylphenyl)porphyrin and OR^- = OPh^-, OCH_2Ph^-, or $OCH(CH_3)_2^-$ were investigated in methylene chloride. The reduction of (TMP)$FeOCH_3$ or (TMP)FeOH in CH_2Cl_2, 0.1 M TBAP occurs via an initial quasi-reversible one-electron-transfer step at $E_{1/2}$ = -0.86 V. A second reduction of $[(TMP)FeOH]^-$ or $[(TMP)FeOCH_3]^-$ is not observed but reduction of (TMP)Fe is observed at $E_{1/2}$ = -1.20 V after dissociation of the anionic ligand. The initial oxidations of (TMP)FeOH and (TMP)$FeOCH_3$ occur at $E_{1/2}$ = 0.98 V in CH_2Cl_2, 0.1 M TBAP to generate $[(TMP)FeOCH_3]^+$ and $[(TMP)FeOH]^+$. These cationic species can be stabilized at low temperature, but at room temperature one or more chemical reactions occur to generate either (TMP)$FeClO_4$ or (TMP)FeCl, both of which undergo two oxidations at ~1.1 and 1.5 V vs. SCE. Thin-layer spectroelectrochemistry was carried out at both room temperature and low temperature in order to characterize the products of each electrochemical and chemical reaction. Steady-state voltammograms were also obtained at a microelectrode in CH_2Cl_2, 0.3 M TBAP and showed one reduction and two oxidations of (TMP)FeOH and (TMP)$FeOCH_3$. All three processes had equal currents, consistent with the addition or abstraction of a single electron at $E_{1/2}$ = -0.95, +1.00, and +1.50 V. The electrochemical and spectroelectrochemical data were combined to give a self-consistent mechanism for oxidation and reduction of the investigated complexes.

Introduction

(TMP)FeOH and (TMP)$FeOCH_3$ (where TMP is the dianion of tetrakis(2,4,6-trimethylphenyl)porphyrin have been characterized by UV-visible, ESR, and ^1H NMR spectroscopy.[1,2] These complexes cannot form μ-oxo dimers, as is the case of (TPP)FeOH and (TPP)$FeOCH_3$ (where TPP = the dianion of tetraphenylporphyrin). Both Fe(III) TMP complexes exist as undissociated five-coordinate high-spin species in toluene or methylene chloride. The electronic absorption spectrum of (TMP)FeOH in toluene has a Soret band at 416 nm, a visible band at 580 nm, and a shoulder at 633 nm.[2] This compares to the absorption spectrum of (TMP)$FeOCH_3$, which in CH_2Cl_2 has a Soret band at 416 nm, a visible band at 580 nm, and a shoulder at 638 nm.[1]

The electrochemistry of simple synthetic metalloporphyrins in nonaqueous media has been recently reviewed.[3] Four recent communications have also been published on the electrochemical oxidation of (TMP)FeOH and (TMP)$FeOCH_3$ under different solution conditions,[5,6-8] but the data and interpretations in these four communications are not internally self-consistent as to the number of electrons transferred in the first electrooxidation step and the axially coordinated ligands on the product of the electrode reactions. Thus, the electrochemistry of (TMP)FeOH and (TMP)$FeOCH_3$ was reinvestigated in this present study, which also reports the first detailed reductive properties of these two complexes. This paper also presents data on the oxidation and reduction of (TMP)FeOR where OR^- = OPh^-, OCH_2Ph^-, and $OCH(CH_3)_2^-$ as well as the electrochemistry of (TMP)$FeClO_4$, (TMP)FeCl, and (TPP)$FeOCH_3$ in CH_2Cl_2, 0.1 M (TBA)ClO_4 containing excess axial ligand at both ambient and low temperatures.

The addition of (TBA)OH to (TMP)FeOH or $NaOCH_3$ to (TMP)$FeOCH_3$ results in formation of a six-coordinate Fe(III) complex, as shown by eq 1 where OR^- = OH^- or OCH_3^-. A

$$(TMP)FeOR + OR^- \rightleftarrows [(TMP)Fe(OR)_2]^- \quad (1)$$

similar ligand addition reaction occurs when $NaOCH_3$ is added to (TPP)FeCl to generate low-spin $[(TPP)Fe(OCH_3)_2]^-$.[4] This reaction is about 50% complete in Me_2SO containing a 10-fold excess of $NaOCH_3$. $[(TPP)Fe(OCH_3)_2]^-$ has been characterized in 99:1 v/v Me_2SO/MeOH mixtures as having absorption bands at 438 (Soret band), 550, 597, and 638 nm. Me_2SO competes with OCH_3^- for binding to the Fe(III) complexes. This is not the case in CH_2Cl_2, where pure OCH_3^--bound complexes may be formed in the presence of slight excess of anion.

The stoichiometric binding of two OCH_3^- anions by oxidized (TMP)$Fe(ClO_4)_2$ is also virtually complete at low temperature.[1] This ligand-exchange reaction is given by eq 2.

$$(TMP)Fe^{III}(ClO_4)_2 + 2OCH_3^- \rightleftarrows (TMP)Fe^{IV}(OCH_3)_2 + 2ClO_4^- \quad (2)$$

Both five- and six-coordinate OCH_3^- complexes may be formed at room temperature, and several electrode reactions between methoxy-bound Fe(III) and Fe(IV) TMP complexes are possible depending upon the actual species in solution. The fact that both $(TMP)Fe^{III}OR$ and $(TMP)Fe^{IV}(OR)_2$ exist in CH_2Cl_2 containing low OR^- concentrations enables evaluation of the electrode reaction given in eq 3. An electrode reaction between bisligated Fe(III)

$$(TMP)FeOR + OR^- \rightleftarrows (TMP)Fe(OR)_2 + e^- \quad (3)$$

and bisligated Fe(IV) can also occur in the presence of excess OR^-. This reaction is given by eq 4. This latter electrode reaction was

$$[(TMP)Fe(OR)_2]^- \rightleftarrows (TMP)Fe(OR)_2 + e^- \quad (4)$$

not investigated in the present report due to complications in the electrochemistry that occur upon the addition of excess methanol or water, which is present in solutions of OR^-.

Experimental Section

Chemicals. $(TMP)H_2$,[9] (TMP)FeCl,[10] (TMP)FeOH,[2] and (TMP)$FeOCH_3$[1] were synthesized according to literature methods. The procedure used for the synthesis of (TMP)FeOR where R = Ph, CH_2Ph, and $CH(CH_3)_2$ was similar to procedures for synthesis of (TMP)$FeOCH_3$.[1] The purities of all compounds were checked by electronic absorption and ^1H NMR spectroscopy and were in good agreement with data in the literature.

All results are reported in dichloromethane (CH_2Cl_2) that was distilled prior to use over calcium hydride under nitrogen. The supporting electrolyte, tetra-*n*-butylammonium perchlorate ((TBA)ClO_4), was recrystallized from ethyl acetate/hexane mixtures. Tetra-*n*-butylammonium

(1) Groves, J. T.; Quinn, R.; McMurry, T. J.; Nakamura, M.; Lang, G.; Boso, B. *J. Am. Chem. Soc.* **1985**, *107*, 354.
(2) Cheng, R.-J.; Latos-Grazynski, L.; Balch, A. L. *Inorg. Chem.* **1982**, *21*, 2412.
(3) Kadish, K. M. *Prog. Inorg. Chem.* **1986**, *34*, 435-605.
(4) (a) Otsuka, T.; Ohya, T.; Sato, M. *Inorg. Chem.* **1985**, *24*, 776. (b) Otsuka, T.; Okya, T.; Sato, M. *Inorg. Chem.* **1984**, *23*, 1777.
(5) Groves, J. T.; Gilbert, J. A. *Inorg. Chem.* **1986**, *25*, 123.
(6) Calderwood, T. S.; Lee, W. A.; Bruice, T. C. *J. Am. Chem. Soc.* **1985**, *107*, 8272.
(7) Calderwood, T. S.; Bruice, T. C. *Inorg. Chem.* **1986**, *25*, 3722.
(8) Lee, W. A.; Calderwood, T. S.; Bruice, T. C. *Proc. Natl. Acad. Sci. U.S.A.* **1985**, *82*, 4301.
(9) Groves, J. T.; Nemo, T. E. *J. Am. Chem. Soc.* **1983**, *105*, 6247.
(10) Adler, A. D.; Longo, F. R.; Kampas, F.; Kim, J. *J. Inorg. Nucl. Chem.* **1970**, *32*, 2443.

0020-1669/87/1326-4360$01.50/0

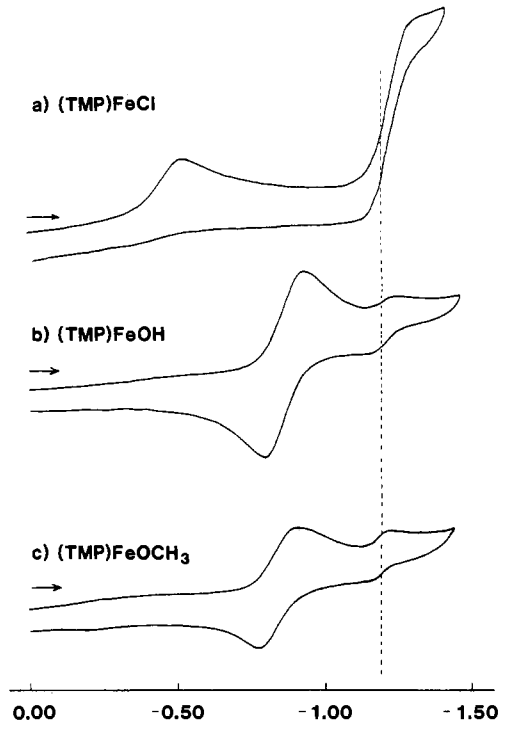

Figure 1. Cyclic voltammograms illustrating the reduction of (a) (TMP)FeCl, (b) (TMP)FeOH, and (c) (TMP)FeOCH$_3$ in CH_2Cl_2, 0.1 M (TBA)ClO_4. Scan rate = 0.20 V/s.

hydroxide ((TBA)OH) was purchased from Fluka as pure grade and was present as 1.5 M (40%) in water. NaOR was synthesized by the reaction of sodium metal and the corresponding alcoholate which was either distilled prior to use or dissolved in freshly distilled benzene, similar to the method described by Groves.[1]

Instrumentation. All electrochemical measurements were performed by using a three-electrode configuration. Conventional voltammograms were obtained with a platinum-wire counter electrode, an IBM saturated calomel electrode, and a gold working electrode. Cyclic voltammetric measurements were made with a BAS 100 electrochemistry system. Low-temperature cyclic voltammetry experiments were carried out by immersing the electrochemical cell in an appropriate dry ice/solvent mixture. The temperature of the solution was measured with an Omega Electronic Model 660 digital thermocouple.

Microvoltammetric experiments were carried out in a well-grounded Faraday cage with a home-built potentiostat that was constructed with LF357N operational amplifiers (National Semiconductor) as described in the literature.[11] A PAR Model 175 universal programmer or a Hewlet Packard 3310B function generator was used to provide the voltage scan. A Textronic Model 5111 storage oscilloscope was used to record voltammograms. The micro working electrode was Pt and was constructed by sealing a 25-μm-diameter platinum wire (Johnson-Mathey, Inc.) into Pyrex tubing. The electrode surface was initially polished with fine sandpaper and carefully finished with a diamond polishing compound (Bioanalytical Systems, Inc.). A homemade aqueous SCE electrode was used as reference electrode and was separated from the bulk solution by an asbestos-tipped frit. All potentials in this paper are reported vs SCE.

Time- and potential-resolved thin-layer spectra were obtained with a Tracor Northern TN-1710 multichannel analyzer using a vacuum-tight thin-layer spectroelectrochemical cell with a doublet platinum-gauze working electrode.[12] This cell was modified in that a light transparent jacket covered the cell body. A similar cell was used for low-temperature experiments and was immersed in a dry ice/solvent mixture that was in a dewar.

Results and Discussion

Electroreduction of (TMP)FeOH and (TMP)FeOCH$_3$. Cyclic voltammograms illustrating the reduction of (TMP)FeCl, (TMP)FeOH, and (TMP)FeOCH$_3$ in CH_2Cl_2, 0.1 M (TBA)ClO_4 are shown in Figure 1. The (TMP)$FeClO_4$ complex (not shown in the figure) is reduced at 0.16 and −1.11 V while (TMP)FeCl (Figure 1a) has reductions at $E_{pc} = -0.49$ V and $E_{1/2} \approx -1.2$ V. The first reduction corresponds to an Fe(III)/Fe(II) process, and the second, to an Fe(II)/Fe(I) transition. The TMP macrocycle has increased basicity with respect to that of TPP, and thus potentials for oxidation or reduction of (TMP)$FeClO_4$ and (TMP)FeCl are negatively shifted by 0.08–0.20 V from potentials for the oxidation or reduction of (TPP)FeCl and (TPP)$FeClO_4$ in CH_2Cl_2.

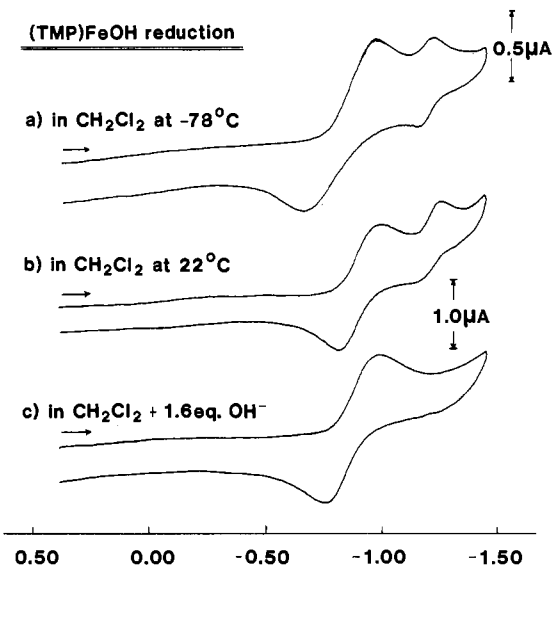

Figure 2. Cyclic voltammograms illustrating the reduction of (TMP)FeOH in CH_2Cl_2, 0.1 M (TBA)ClO_4: (a) −78 °C; (b) 22 °C; (c) 22 °C in CH_2Cl_2 solutions containing 1.6 equiv of (TBA)OH.

Both (TMP)FeOH (Figure 1b) and (TMP)FeOCH$_3$ (Figure 1c) exhibit a one-electron quasi-reversible reduction at $E_{1/2} = -0.86$ V. The second reduction of (TMP)FeOH and (TMP)FeOCH$_3$ occurs at $E_{1/2} = -1.20$ and −1.21 V, which are identical with the $E_{1/2}$ values for the second reduction of (TMP)$FeClO_4$ and (TMP)FeCl (Figure 1). The peak currents for the second reduction of (TMP)FeOH and (TMP)FeOCH$_3$ are also significantly smaller than the peak currents for the first reduction of the complex. Both of these facts suggest that (TMP)Fe is generated after electroreduction of (TMP)FeOH or (TMP)FeOCH$_3$ and that the overall electrode reactions in CH_2Cl_2 are given by eq 5–7 where $OR^- = OH^-$ or OCH_3^-.

$$(TMP)FeOR + e^- \rightleftarrows [(TMP)FeOR]^- \quad E_{1/2} = -0.86 \text{ V} \quad (5)$$

$$[(TMP)FeOR]^- \rightleftarrows (TMP)Fe + OR^- \quad (6)$$

$$(TMP)Fe + e^- \rightleftarrows [(TMP)Fe]^- \quad E_{1/2} = -1.21 \text{ V} \quad (7)$$

The above sequence of steps is supported by cyclic voltammetry of (TMP)FeOH in the presence and absence of excess OH^- (Figure 2). The initial voltammogram of (TMP)FeOH contains two reduction processes between −78 (Figure 2a) and +22 °C (Figure 2b). However, upon addition of excess OH^-, the equilibrium of reaction 6 is displaced toward the left and a single reversible reduction is obtained in CH_2Cl_2 containing 1.6 equiv of (TBA)OH. This voltammogram is shown in Figure 2c.

The sequence of steps shown by reactions 5–7 is also supported by variable-temperature spectroelectrochemistry of (TMP)FeOCH$_3$ and (TMP)FeOH in CH_2Cl_2. Thin-layer spectra recorded at −60 °C during reduction of (TMP)FeOH are shown in Figure 3a. The final spectrum has a Soret band at 447 nm, a small band at 535 nm, and two higher intensity visible bands at 578 and 619 nm. There are isobestic points at 395, 430, 470, 590, and 607 nm. The final spectra of $[(TMP)FeOH]^-$ and

(11) Howell, J. O.; Wightman, R. M. *Anal. Chem.* **1984**, *56*, 524.
(12) Lin, X. Q.; Kadish, K. M. *Anal. Chem.* **1985**, *57*, 1498.

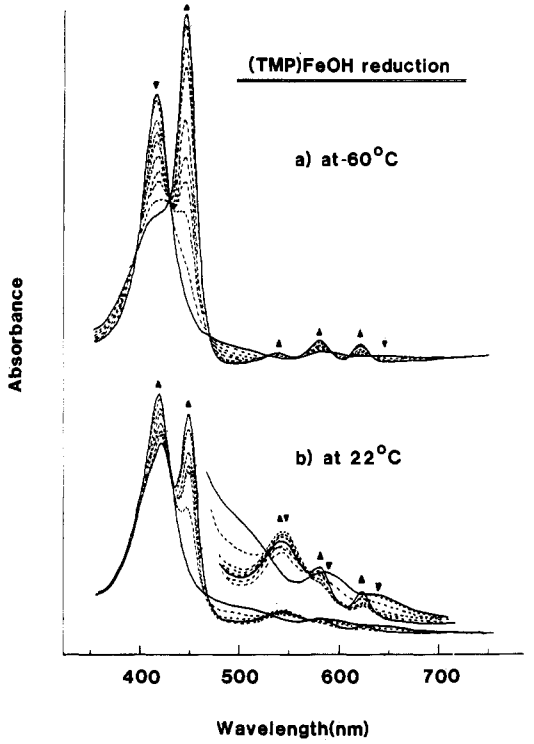

Figure 3. Thin-layer spectra recorded during the first reduction of (TMP)FeOH in CH_2Cl_2, 0.1 M $(TBA)ClO_4$: (a) for 1 min at −0.96 V in solutions at −60 °C; (b) for 7 min at −1.0 V in solutions at 22 °C.

Table I. Spectral Properties of Four- and Five-Coordinate Fe(II) Porphyrins

compd	solvent	temp	λ_{max}, nm				
(TMP)FeOH	CH_2Cl_2	−60 °C		447	535	578	619
redn product		22 °C	419	445	537	576	618
$(TMP)FeOCH_3$	CH_2Cl_2	−60 °C		446	530	576	617
redn product		22 °C	412	442	530	574	617
$[(TPP)FeX]^-$ [a]	$EtCl_2$	ambient		441	530 (sh) [b]	570	610
(TPP)Fe [a]	$EtCl_2$	ambient	417	443	537		

[a] Reference 13. [b] sh = shoulder.

$[(TMP)FeOCH_3]^-$ are similar to each other and to spectra of $[(TPP)FeX]^-$ complexes that have bands at 441, 570, and 610 nm and a shoulder at 530 nm.[13] A similar spectrum is also obtained after reduction of $(TMP)FeOCH_3$ in CH_2Cl_2 solutions containing 2 equiv of $NaOCH_3$. These spectral details are summarized in Table I, which also lists the spectra of four-coordinate $(TPP)Fe^{II}$.

The room-temperature spectrum of electroreduced (TMP)FeOH is shown in Figure 3b and suggests a mixture of four- and five-coordinate Fe(II) porphyrins. The electronic absorption spectrum is similar to spectra of electroreduced (TPP)FeX, where mixtures of (TPP)Fe and $[(TPP)FeX]^-$ are generated.[13] However, the presence of some $[(TMP)Fe(OH)_2]^{2-}$ and $[(TMP)Fe(OCH_3)_2]^{2-}$ under the solution conditions of Figure 3b is also possible; $[(TPP)Fe(OCH_3)_2]^{2-}$ has a split Soret band at 417 and 450 nm[4] and three visible bands at wavelengths similar to those of $[(TPP)FeX]^-$.[13]

Autoreduction of (TMP)FeOR. Autoreductions of $[(P)Fe(OCH_3)_2]^-$ have been reported in dimethyl sulfoxide,[3,14] where $[(P)Fe(OCH_3)_2]^{2-}$ is the generated Fe(II) product. Degassed (TMP)FeOH and $(TMP)FeOCH_3$ are also light sensitive in CH_2Cl_2 containing OR^-. This is shown in Figure 4, which illustrates the spectra of 5.8×10^{-4} M (TMP)FeOH in CH_2Cl_2 + 10^{-3} M (TBA)OH during exposure to a tungsten light source.

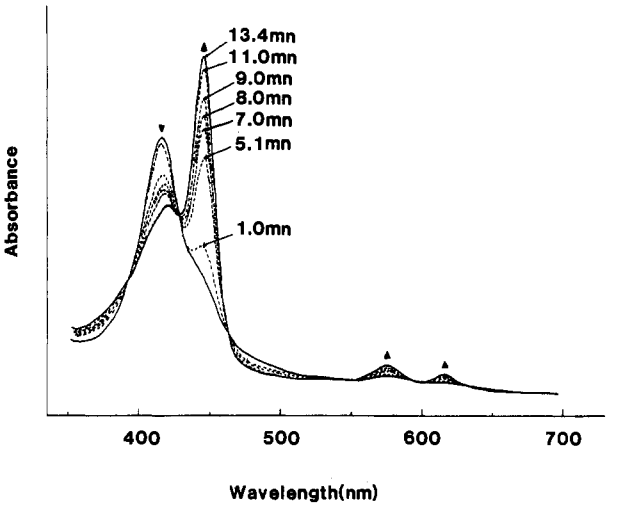

Figure 4. Time-resolved electronic absorption spectra of 5.8×10^{-4} M (TMP)FeOH in degassed CH_2Cl_2 containing 1×10^{-3} M (TBA)OH. The sample was exposed to a tungsten light source between measurements.

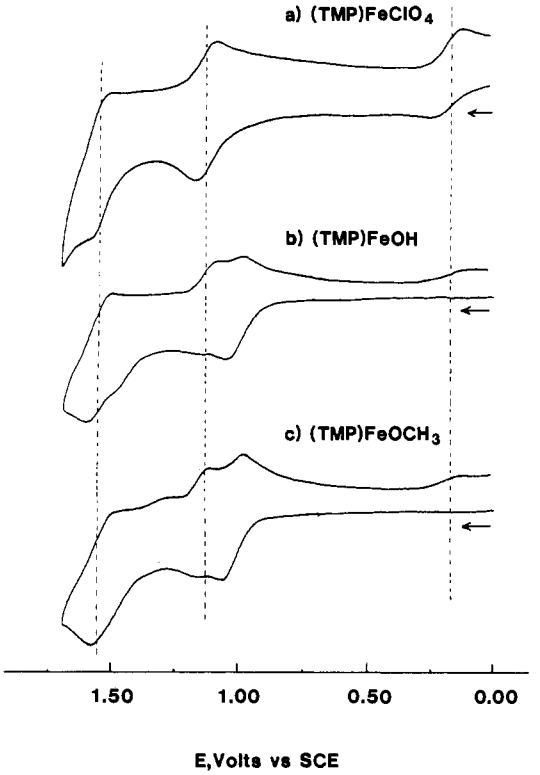

Figure 5. Cyclic voltammograms showing the oxidation of (a) (TMP)$FeClO_4$, (b) (TMP)FeOH, and (c) $(TMP)FeOCH_3$ in CH_2Cl_2, 0.1 M $(TBA)ClO_4$. Scan rate = 0.20 V/s.

The final spectrum is similar to that of $[(TMP)FeOH]^-$. The same final spectrum is also obtained in toluene after exposure of (TMP)FeOH or $(TMP)FeOCH_3$ to visible light, but in this solvent the time required to generate the reduced species is longer.

The autoreduction only involves the central iron atoms, and no other changes in the macrocycle occur upon exposure to light. This was verified by the fact that the initial spectrum of (TMP)FeOH or $(TMP)FeOCH_3$ could be regenerated upon exposure of the photoreduced complex to the atmosphere, thus confirming that the spectral changes are due only to a reversible redox process.

Electrooxidation of (TMP)FeOH and $(TMP)FeOCH_3$. Cyclic voltammograms illustrating the oxidation of $(TMP)FeClO_4$, (TMP)FeOH, and $(TMP)FeOCH_3$ in CH_2Cl_2 are shown in Figure 5. $(TMP)FeClO_4$ is reduced to (TMP)Fe at $E_{1/2}$ = 0.16 V and

(13) Kadish, K. M.; Rhodes, R. K. *Inorg. Chem.* **1983**, *22*, 1090.
(14) Chang, C. K.; Dolphin, D. *Proc. Natl. Acad. Sci. U.S.A.* **1976**, *73*, 3338.

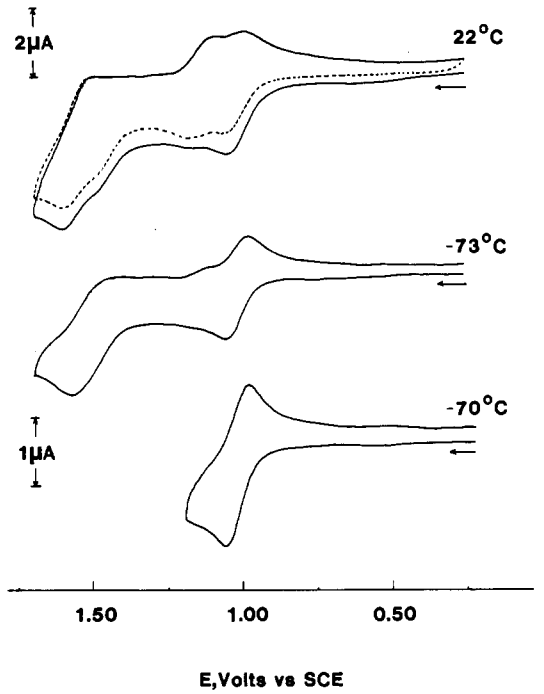

Figure 6. Cyclic voltammograms illustrating the first (—) and second (---) potential scan during oxidation of (TMP)FeOH at 22, −73, and −70 °C (first oxidation only).

oxidized to (TMP)Fe(ClO_4)$_2$ and [(TMP)Fe(ClO_4)$_2$]$^+$ at $E_{1/2}$ = 1.09 and 1.49 V. This is shown in Figure 5a. In contrast, (TMP)FeOH (Figure 5b) and (TMP)FeOCH$_3$ (Figure 5c) have three oxidations at 0.98, 1.10, and either 1.52 or 1.50 V. These room-temperature voltammograms are virtually identical with those reported in the literature.[7,8]

Under our experimental conditions (TMP)FeOH has an additional small anodic peak at $E_{pa} \approx 1.46$ V while (TMP)FeOCH$_3$ has an additional cathodic peak at $E_{pc} \approx 1.25$ V. On the reverse scan, both compounds show a cathodic peak close to 0.16 V. The reduction peak at ≈ 0.16 V is coupled to a corresponding anodic peak, which is not present on the original positive potential scan. This peak is clearly due to the reduction of electrogenerated (TMP)FeClO_4 and the reoxidation of (TMP)Fe, which is formed after the addition of one electron to this complex.

The second oxidation of (TMP)FeOH and (TMP)FeOCH$_3$ occurs at $E_{1/2}$ = 1.10 V and may be compared with the first oxidation (TMP)FeClO_4, which occurs at $E_{1/2}$ = 1.09 V (see dashed line in Figure 5). The second oxidation of (TMP)FeOH and (TMP)FeOCH$_3$ is well-defined at room temperature but almost completely disappears at low temperature. This is illustrated in Figure 6. As seen in this figure, the second potential scan in the oxidation of (TMP)FeOH at 22 °C indicates an increase in current for the oxidation process at 1.10 V. However, this process disappears at low temperature. Also, the voltammogram becomes more reversible if the sweep is reversed after the first oxidation. These data suggest that the electrode reaction at 1.10 V is due to oxidation of a product formed during a chemical reaction following the first electrooxidation of (TMP)FeOH. The most likely product is (TMP)FeClO_4, as suggested by the voltammograms in Figure 5.

Figure 7 illustrates cyclic voltammograms of (TMP)FeCl and solution-generated (TMP)FeOCH$_3$, and [(TMP)Fe(OCH$_3$)$_2$]$^-$ in CH_2Cl_2 containing various concentrations of $NaOCH_3$. The cyclic voltammogram of (TMP)FeCl in CH_2Cl_2, 0.1 M (TBA)ClO_4 (Figure 7a) exhibits two one-electron reversible oxidations at 1.09 and 1.49 V. The first oxidation product is an iron(III) cation radical. However, a new oxidation/reduction process appears at ~0.98 V after the addition of 0.6 equiv of $NaOCH_3$ (Figure 7b). This process has been assigned as corresponding to an Fe(III)/Fe(IV) reaction.[8] The currents for the wave at 0.98 V increase in intensity with further additions of $NaOCH_3$ (see Figure 7c–e),

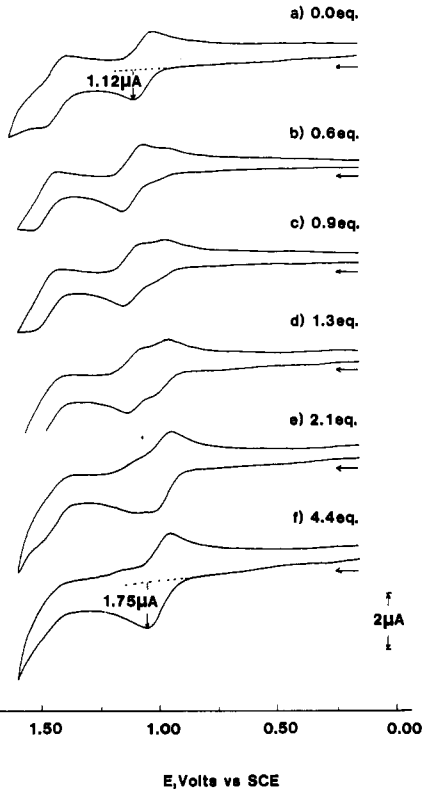

Figure 7. Cyclic voltammograms of (TMP)FeCl in CH_2Cl_2, 0.1 M (TBA)ClO_4 containing the following equivalents of $NaOCH_3$: (a) 0; (b) 0.6; (c) 0.9; (d) 1.3; (e) 2.1; (f) 4.4.

and in the presence of 1.3 equiv of $NaOCH_3$ (Figure 7d) the cyclic voltammogram is almost identical with that for (TMP)FeOCH$_3$ (see Figure 5c). The only difference in these two figures is in the Fe(III)/Fe(II) regions of the voltammograms. ((TMP)FeClO_4 is reduced at 0.16 V, but this species cannot be formed since Cl^- is present in solution from the initial (TMP)FeCl.) The first oxidation of (TMP)FeCl at 1.10 V continues to decrease after the addition of 2.1 equiv (Figure 7e) and totally disappears when 4.4 equiv of $NaOCH_3$ is added to solution.

The ESR spectrum of the solution in Figure 7 was taken before and after the addition of $NaOCH_3$. Only traces of the low-spin Fe(III) form are present in solutions containing 4.4 equiv of OCH_3^-. Thus, under these conditions the overall electrode reaction can be written as

$$(TMP)Fe^{III}(OCH_3) + OCH_3^- \rightleftarrows (TMP)Fe^{IV}(OCH_3)_2 + e^- \quad (8)$$

This electrode reaction differs from that for the oxidation of (TMP)FeOCH$_3$ in the absence of excess OCH_3^-. Under these conditions the initial one-electron oxidation will generate (TMP)Fe(OCH$_3$)ClO_4.

Thin-layer electronic absorption spectra were recorded during controlled-potential oxidation of (TMP)FeOCH$_3$ in CH_2Cl_2, 0.1 M (TBA)ClO_4. When the oxidation was carried out at ambient temperature (Figure 8a), the Soret band initially decreased while a band at 510 nm appeared. As the oxidation proceeded, the band at 510 nm decreased in intensity and the Soret band shifted toward lower wavelengths, indicating the formation of a cation radical.

A cation radical is also formed during oxidation of (TMP)FeOCH$_3$ at low temperature (Figure 8b). However, under these conditions there was not a band at 510 nm, thus suggesting either that the radical cation formed at low temperature is different from the one formed at ambient temperature or that two different species are formed as a function of temperature.

Figure 9 shows the initial and final spectra obtained during oxidation of (TMP)FeOH in CH_2Cl_2 at ambient and low temperature. Oxidation of (TMP)FeOH at −64 °C gives a smaller 510-nm band than oxidation at room temperature. The band at

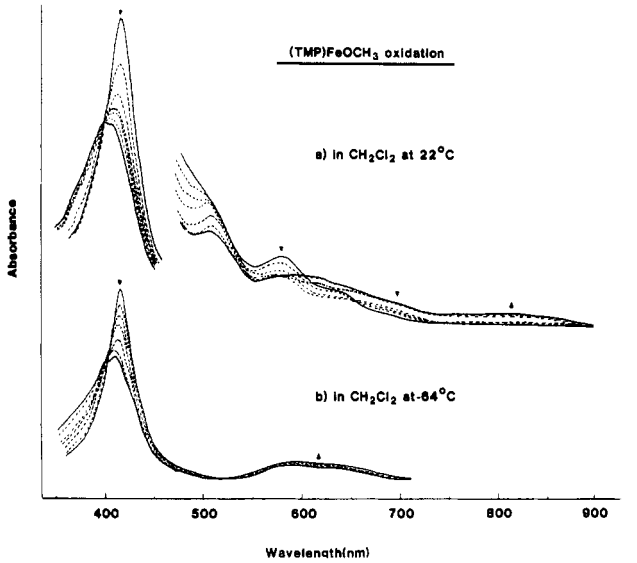

Figure 8. Thin-layer spectra recorded during the controlled-potential oxidation of $(TMP)FeOCH_3$: (a) for 1 min at 1.1 V in CH_2Cl_2, 0.1 M $(TBA)ClO_4$ at 22 °C; (b) for 1 min at 1.2 V in CH_2Cl_2, 0.1 M $(TBA)ClO_4$ at −64 °C.

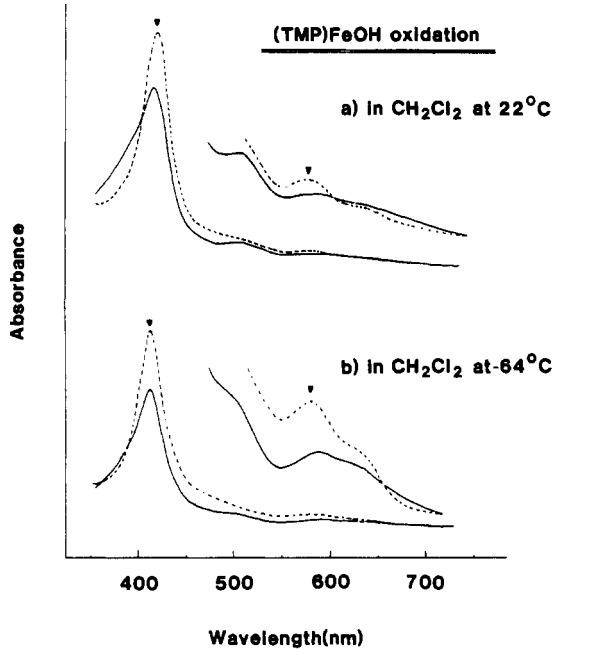

Figure 9. Initial (---) and final (—) spectra recording during the controlled-potential oxidation of (TMP)FeOH: (a) at 1.1 V in CH_2Cl_2, 0.1 M $(TBA)ClO_4$ at 22 °C; (b) at 1.2 V in CH_2Cl_2 solutions at −64 °C.

510 nm may be assigned as due to $(TMP)Fe(OH)ClO_4$, or alternatively, it may be due to $(TMP)FeClO_4$ or (TMP)FeCl, both of which have absorption bands in this region. Similar bands were obtained for electrooxidized $(TMP)FeOCH_3$ and (TMP)FeOH in CH_2Cl_2 solutions, and the cyclic voltammetric data suggest that $(TMP)FeClO_4$ is the product of the electrooxidation.

Room-temperature oxidations of (TMP)FeOH and $(TMP)FeOCH_3$ in the presence of excess ligand (Figure 10a) give spectra similar to those for unoxidized (TMP)FeOR but differ in that there is a decrease of intensity in both the Soret band and visible region of the spectrum. However, oxidation of the same solution at low temperature gives a different UV–visible spectrum. This spectrum (Figure 10b) is identical with the spectrum reported by Groves for $(TMP)Fe^{IV}(OCH_3)_2$.[1]

The low-temperature spectrum of electrooxidized (TMP)FeOH in solutions containing excess aqueous (TBA)OH is similar to the spectrum reported by Balch and LaMar for (TmTP)Fe(O)(*N*-MeIm) in toluene.[15] The ESR spectra of $[(TMP)Fe(OH)_2]^-$ and

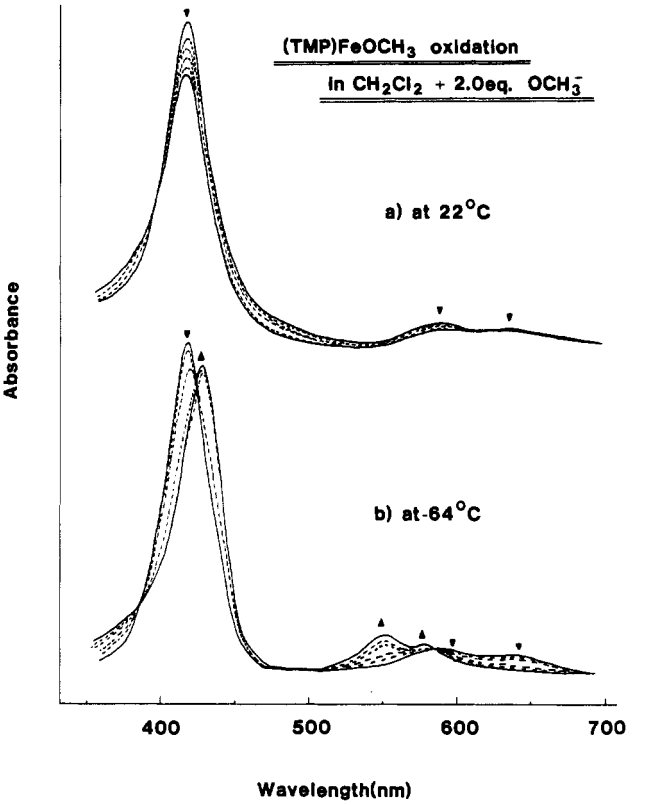

Figure 10. Thin-layer spectra recorded during the oxidation of $(TMP)FeOCH_3$ in CH_2Cl_2 containing 0.1 M $(TBA)ClO_4$ and 2 equiv of $NaOCH_3$: (a) oxidation of 22 °C solution at 1.1 V; (b) oxidation of −64 °C solution at 1.2 V.

Scheme I

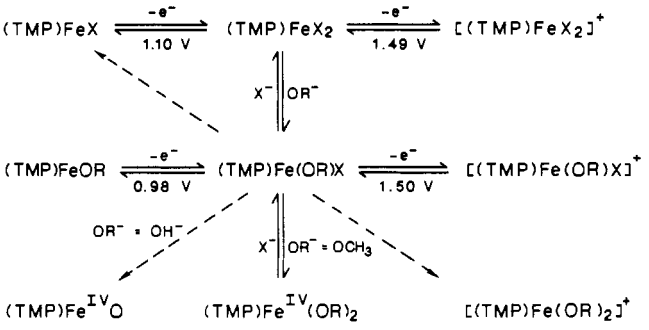

$[(TMP)Fe(OCH_3)_2]^-$ are similar at 120 K, and similar UV–visible spectra are also obtained in CH_2Cl_2 when 2 equiv of $NaOCH_3$ or TBAOH is added to chemically or electrochemically synthesized $(TMP)Fe(ClO_4)_2$ at low temperature. However, the initial spectrum of (TMP)FeOH or $(TMP)FeOCH_3$ is again obtained when the temperature of this solution is raised to 22 °C. A similar result was reported by Groves.[1]

The above electrochemical and spectroelectrochemical data indicate that several different types of electrode reactions may occur in CH_2Cl_2 depending upon the type and concentration of oxyanion in solution. For example, (TMP)FeOH may be oxidized to $(TMP)Fe^{IV}O$ without excess OH^-. On the other hand, quantitative generation of $(TMP)Fe^{IV}(OCH_3)_2$ from $(TMP)FeOCH_3$ is not possible in the absence of excess OCH_3^-. Under these conditions the most likely initial step in the electrooxidation corresponds to the reaction given by eq 9. The electrogenerated

$$(TMP)FeOCH_3 + ClO_4^- \rightleftarrows (TMP)Fe(OCH_3)ClO_4 + e^- \quad (9)$$

$(TMP)Fe(OCH_3)ClO_4$ may or may not contain Fe(IV), but this

(15) Chin, D. H.; Balch, A. L.; LaMar, G. N. *J. Am. Chem. Soc.* **1980**, *102*, 1446.

Table II. Maximum Wavelengths for the Product Formed in the Reaction between (TMP)Fe(ClO$_4$)$_2$ and ~2 equiv of NaOR at Low and Ambient Temperatures in CH_2Cl_2

suggested oxidn state[a]	added ligand	temp °C	λ_{max}, nm				
Fe(IV)	$NaOCH_2Ph$	−60	422	546	579		
	$NaOCH(CH_3)_2$	−56	419	545	578		
	$NaOCH_3$	−51	423	547	578		
	(TBA)OH	−47	421	566	603		
Fe(III)	$NaOCH_2Ph$	22	421	581 (sh)[b]	634 (sh)		
	$NaOCH(CH_3)_2$	22	419	578	629 (sh)		
	$NaOCH_3$	22	417	580	634 (sh)		
	(TBA)OH	22	419	585	633 (sh)		
Fe(III)	NaOPh	−46	420	493	555	635	637 (sh)
		22	417	489	552		655 (sh)

[a] The complex spectrally characterized should be (TMP)Fe(OR)$_2$. Oxidation-state assignment is based on analogy with low-temperature spectra of (TMP)Fe(OCH$_3$)$_2$ and (TMP)FeO. [b] sh = shoulder.

compound can easily disproportionate to generate equimolar mixtures of [(TMP)Fe^{IV}(OCH$_3$)$_2$]$^+$ and (TMP)Fe^{III}ClO$_4$. Thus, one proposed electrooxidation mechanism for (TMP)FeOH and (TMP)FeOCH$_3$ is shown in Scheme I, where OR$^-$ = OH$^-$ or OCH$_3^-$ and X = ClO$_4^-$ or Cl$^-$. Scheme I is consistent with the electrochemical and spectroscopic data that suggest conversion of (TMP)Fe(OR)X to (TMP)FeClO$_4$ in the absence of added OH$^-$ or OCH$_3^-$ ligand. This conversion may occur via a ligand-exchange reaction to give (TMP)Fe(ClO$_4$)$_2$ and (TMP)Fe(OR)$_2$ or via a disproportionation reaction to give (TMP)FeClO$_4$ and [(TMP)Fe(OR)$_2$]$^+$. Any highly oxidized [(TMP)Fe^{IV}(ClO$_4$)$_2$]$^+$ generated from (TMP)Fe(OR)ClO$_4$ at 0.98 V would be rereduced to (TMP)FeClO$_4$ before reoxidation at +1.10 V or alternatively could react with the CH_2Cl_2 solvent to generate Cl$^-$ with the ultimate formation of (TMP)FeCl.

The formation of (TMP)Fe(OCH$_3$)$_2$ or (TMP)FeO can also be accomplished by the addition of OR$^-$ to (TMP)Fe(ClO$_4$)$_2$ at low temperature.[1,5] The oxo- and methoxy-bound species have different spectra consistent with the different axial binding modes of the two Fe(IV) complexes. A loss of OCH$_3^-$ is also observed upon oxidation of (TPP)FeOCH$_3$, and this would explain the formation of some μ-oxo dimer.[8] Kinetic studies have shown that OH$^-$ ligation is a first step in the formation of μ-oxo dimer and that this is followed by the reaction shown in eq 10.[16-18]

$$(TPP)FeOH + [(TPP)Fe]^+ \rightarrow [(TPP)Fe]_2O + H^+ \quad (10)$$

Finally, the generation of (TMP)FeX where X$^-$ = Cl$^-$ or ClO$_4^-$ from [(TMP)FeOR]$^+$ does not contribute to changes in the current–voltage curves when oxidations are carried out at a microelectrode. This is shown in Figure 11, which illustrates room-temperature, steady-state voltammograms for oxidation and reduction of (TMP)FeOH and (TMP)FeOCH$_3$ in CH_2Cl_2, 0.3 M TBAP. As seen in this figure, both Fe(III) complexes are reduced by one single-electron-transfer step at $E_{1/2}$ = −0.95 V and oxidized by two single-electron-transfer steps at $E_{1/2}$ = 1.0 and 1.5 V. The currents for all three processes of each compound are identical within experimental error. Under the conditions of these experiments, the products of the chemical reactions following reduction (see Figures 1 and 2) and oxidation (see Figures 5–7) of (TMP)FeOH and (TMP)FeOCH$_3$ are not voltammetrically observed. Thus, one can easily differentiate oxidation or reduction waves due to the species actually in solution from waves that are due to products generated by one or more coupled homogeneous reactions.

Investigation of Other (TMP)FeOR Complexes. The monomeric iron(IV) porphyrin complexes characterized to date contain strong coordinating ligands such as OH$^-$ or OCH$_3^-$. However, other donating ligands should also be able to stabilize a high oxidation state of the metal at low temperature. Three possibilities are OPh$^-$, OCH$_2$Ph$^-$, and OCH(CH$_3$)$_2^-$. The OPh$^-$ and OCH$_2$Ph$^-$ anions are less basic than OH$^-$ and OCH$_3^-$ while OCH(CH$_3$)$_2^-$ is more basic than OCH$_3^-$.

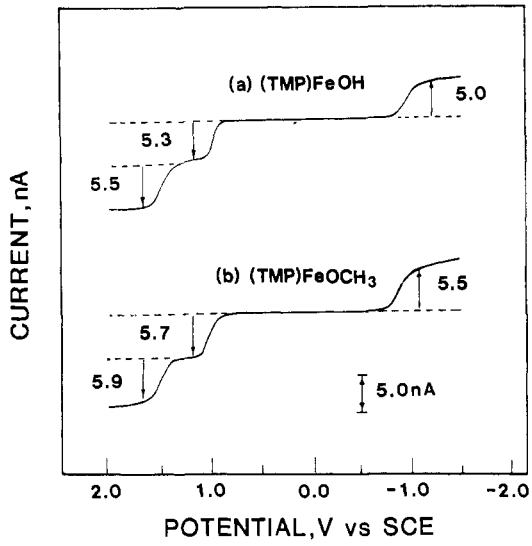

Figure 11. Steady-state voltammograms for the oxidation and reduction of (TMP)FeOH and (TMP)FeOCH$_3$ at a microelectrode in CH_2Cl_2, 0.3 M (TBA)ClO$_4$. Scan rate = 0.05 V/s.

In order to investigate the possible formation of an iron(IV) porphyrin, 2-equiv amounts of each OR$^-$ ligand were added to (TMP)Fe(ClO$_4$)$_2$ at low temperature, after which the spectra were recorded. The spectra were also recorded as the solution was warmed to ambient temperature. These low-temperature and room-temperature spectral data are summarized in Table II.

Different spectra are obtained at low and room temperatures. (TMP)FeOPh shows an electronic absorption spectrum that is different from those of (TMP)FeOH and (TMP)FeOCH$_3$. This compound also does not exhibit a large difference in the spectra between low and high temperatures. This suggests a possible hexacoordination at low temperature but not stabilization of iron(IV).

The OCH$_2$Ph$^-$ and OCH(CH$_3$)$_2^-$ complexes have spectra similar to the OH$^-$ and OCH$_3^-$ derivatives at room temperature. The spectra are also similar to the OCH$_3^-$ derivatives at low temperature, suggesting the formation of an iron(IV) complex under these conditions. This implies that OPh$^-$ is not basic enough to stabilize an iron(IV) at low temperature. This may be due to the fact that the negative charge is too much delocalized.

Pure (TMP)FeOPh, (TMP)FeOCH$_2$Ph, and (TMP)FeOCH(CH$_3$)$_2$ were synthesized and characterized by electronic absorption spectroscopy, ^{1}H NMR spectroscopy, and electrochemistry. All three complexes have NMR spectra similar to those of (TMP)FeOH and (TMP)FeOCH$_3$. The pyrrole proton resonances of the five (TMP)Fe(OR) complexes are between 77.9 and 80.5 ppm; the meta proton resonances are between 11.7 and 12.4 ppm and 10.9 and 11.4 ppm. The NMR shifts clearly differentiate

(16) Fielding, L.; Eaton, G. R.; Eaton, S. S. *Inorg. Chem.* **1985**, *24*, 2309.
(17) More, K. M.; Eaton, G. R.; Eaton, S. S. *Inorg. Chem.* **1985**, *24*, 3698.
(18) Woon, T. C.; Shirazi, A.; Bruice, T. C. *Inorg. Chem.* **1986**, *25*, 3845.

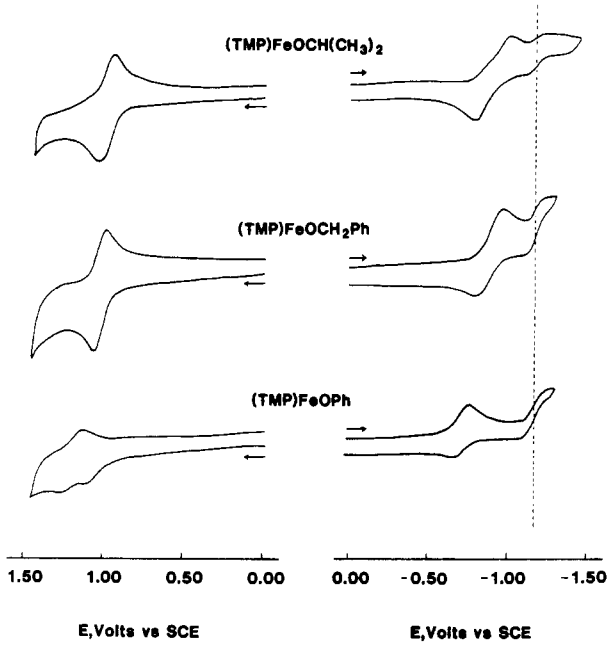

Figure 12. Cyclic voltammograms of (TMP)FeOCH$(CH_3)_2$, (TMP)-FeOCH$_2$Ph, and (TMP)FeOPh in CH_2Cl_2, 0.1 M (TBA)ClO_4.

complexes of (TMP)Fe(OR) from (TMP)FeCl or (TMP)$FeClO_4$, which have meta proton resonances at 16.0, 14.4, and 10.5 ppm, respectively.[1,2]

Figure 12 shows cyclic voltammograms of (TMP)FeOCH-$(CH_3)_2$, (TMP)FeOCH$_2$Ph, and (TMP)FeOPh in the presence of excess coordinating ligand. Half-wave and peak potentials of the (TMP)FeOR complexes are virtually identical with those of (TMP)$FeOCH_3$ and (TMP)FeOH under the same experimental conditions. (TMP)FeOPh has a single anodic peak for the first oxidation, and its reduction potential is shifted positively compared to those of the other alcoholate complexes. This suggests a lower electron density on the metal and indicates that the oxidized product is even less stable than the other complexes.

The first oxidation product can be stabilized at low temperature. The two other alcoholate-bound complexes have essentially the same oxidation behaviors. However, (TMP)FeOCH$(CH_3)_2$ clearly shows a mixture upon reduction. This mixture probably contains [(TMP)FeOCH$(CH_3)_2]^-$, [(TMP)FeOCH$(CH_3)_2]^{2-}$, and (TMP)Fe.

In summary, (TMP)FeOH and (TMP)$FeOCH_3$ have similar physicochemical properties and similar electrochemistries. The only difference between these two complexes is the oxidation products at low temperature in the absence of excess ligand. Similar results are also obtained when other alcoholates are substituted for OH^- or OCH_3^-. The only exception occurs when the axial ligand is not sufficiently electron donating. This is illustrated by (TMP)FeOPh, which is easier to reduce. The electrooxidation product is also unstable, and (TMP)Fe$(OPh)_2$ does not seem to contain iron(IV) at low temprature.

Acknowledgment. The support of the National Institutes of Health (Grant No. GM-25172) is gratefully acknowledged.

Registry No. (TMP)FeOH, 77439-20-4; (TMP)$FeOCH_3$, 93842-72-9; (TMP)FeOPh, 111435-61-1; (TMP)FeOCH$_2$Ph, 111468-45-2; (TMP)FeOCH$(CH_3)_2$, 111435-62-2; (TMP)Fe(ClO_4), 94423-72-0; (TMP)FeCl, 77439-21-5; (TMP)Fe$(OCH_3)_2$, 93862-19-2; (TMP)Fe-$(OCH_3)ClO_4$, 111435-63-3; [(TMP)Fe$(OH)_2]^-$, 111435-64-4; [(TMP)-Fe$(OH_3)_2]^-$, 111435-65-5; (TMP)Fe, 81567-13-7; [(TMP)Fe$(ClO_4)_2]^+$, 111435-60-0; (TMP)Fe$(ClO_4)_2$, 93842-71-8; NaOCH$_2$Ph, 20194-18-7; NaOCH$(CH_3)_2$, 683-60-3; $NaOCH_3$, 124-41-4; (TBA)OH, 2052-49-5; (TBA)ClO_4, 1923-70-2.

Contribution from the Anorganisch-Chemisches Institut der Universität Heidelberg, Im Neuenheimer Feld 270, 6900 Heidelberg, FRG

Synthesis, Molecular Structure, and Tumor-Inhibiting Properties of Imidazolium *trans*-Bis(imidazole)tetrachlororuthenate(III) and Its Methyl-Substituted Derivatives

B. K. Keppler,* W. Rupp, U. M. Juhl, H. Endres, R. Niebl, and W. Balzer

Received August 19, 1986

The synthesis, the molecular structure, and the antitumor activity of ImH$(RuIm_2Cl_4)$ and, in addition, the synthesis and antitumor screening data of three methyl-substituted derivatives as well as the molecular structure of one of these are described in this paper. $[ImH]^+[RuCl_4Im_2]^-$ (**1**): $(C_2H_5N_2)^+(C_6H_8Cl_4N_4Ru)^-$; M_r = 448.13; monoclinic; $C2/c$; a = 13.266 (3), b = 8.047 (1), c = 16.514 (4) Å; β = 112.53 (2)°; V = 1628 Å^3; Z = 4; D_{calcd} = 1.83 g cm^{-3}. The final R_w was 0.029 for 1710 reflections and 106 parameters. $[4\text{-MeImH}]^+[Ru(4\text{-MeIm})_2Cl_4]^-$ (**2**): $(C_4H_7N_2)^+(C_8H_{12}Cl_4N_4Ru)^-$; M_r = 490.21; monoclinic; $P2_1/a$; a = 12.947 (3), b = 10.484 (3), c = 14.170 (4) Å; β = 108.22 (2)°; V = 1827 Å^3; Z = 4; D_{calcd} = 1.78 g cm^{-3}. The final R_w was 0.039 for 2563 reflections and 211 parameters. The antitumor activity was investigated in the P 388 leukemia, the Walker 256 carcinosarcoma, and the intramusculary transplanted sarcoma 180. In the P 388 leukemia model, the lifespan of the animals treated with ImH$(RuIm_2Cl_4)$ was increased up to T/C values of 194%. The activity was in the same range as or was slightly better than in the case of cisplatin, which was tested as a positive control. 5-Fluorouracil was less active compared to this metal complex. The compound showed promising activity also in the Walker 256 carcinosarcoma and the sarcoma 180 models.

The aim of our research in the field of antitumor-active metal complexes is to develop new compounds for the treatment of cancer. Preferably these compounds should be active against those human tumors that cannot be treated sufficiently by standard chemotherapy protocols.[1,2]

Recently, we described a new tumor-inhibiting ruthenium complex, bis(imidazolium) (imidazole)pentachlororuthenate(III), $(ImH)_2(RuImCl_5)$.[3] Now we present the synthesis, molecular structure, and antitumor activity of imidazolium *trans*-bis(imidazole)tetrachlororuthenate(III) and, in addition, the synthesis and antitumor screening data of three methyl-substituted derivatives

* To whom correspondence should be addressed.

(1) Keppler, B. K.; Schmähl, D. *Arzneim.-Forsch.* **1986**, *36*, 1822-1828.
(2) Bischoff, H.; Berger, M. R.; Keppler, B. K.; Schmähl, D. *J. Cancer Res. Clin. Oncol.* **1987**, *113*, 446-450.
(3) Keppler, B. K.; Wehe, D.; Endres, H.; Rupp, W. *Inorg. Chem.* **1987**, *26*, 844-846.

0020-1669/87/1326-4366$01.50/0